Metall. Res. Technol. **118**, 601 (2021)

https://doi.org/10.1051/metal/2021078

Metallurgical Research & Technology

Available online at:
www.metallurgical-research.org

Regular Article

Microstructure and mechanical properties of 15-5 PH stainless steel under different aging temperature

Chunhui Jin[1], Honglin Zhou[2], Yuan Lai[1], Bei Li[1], Kewei Zhang[1], Huiqin Chen[1], and Jinhua Zhao[1,*]

[1] School of Materials Science and Engineering, Taiyuan University of Science and Technology, Taiyuan 030024, PR China
[2] Neusoft Medical Sysems Co., Ltd., Shenyang 110179, PR China

Received: 10 June 2021 / Accepted: 13 September 2021

Abstract. The influence of aging temperature on microstructure and mechanical properties of Cr15Ni5 precipitation hardening stainless steel (15-5 PH stainless steel) were investigated at aging temperature range of 440–610 °C. The tensile properties at ambient temperature of the 15-5 PH stainless steel processed by different aging temperatures were tested, and the microstructural features were further analyzed utilizing optical microscope (OM), transmission electron microscope (TEM), electron backscatter diffraction (EBSD) as well as X-ray diffraction (XRD), respectively. Results indicated the strength of the 15-5 PH stainless steel was firstly decreased with increment of aging temperature from 440 to 540 °C, and then increased with the increment of aging temperature from 540 to 610 °C. The strength and ductility were well matched at aging temperature 470 °C, and the yield strength, tensile strength as well as elongation were determined to be 1170 MPa, 1240 MPa and 24%, respectively. The microstructures concerning to different aging temperatures were overall confirmed to be lath martensite. The strengthening mechanisms induced by dislocation density and the second phase precipitation of Cu-enriched metallic compound under different aging temperatures were determined to be the predominant strengthening mechanisms controlling the variation trend of mechanical properties corresponding to different aging temperatures with respect to 15-5 PH stainless steel.

Keywords: 15-5 PH stainless steel / aging process / strengthening mechanism / lath martensite

1 Introduction

Maraging stainless steel (MSS) characterized by carbon-free or ultra-low carbon has been widely applied in the fields of aerospace, machinery manufacturing and military industries [1–3]. As a typical steel grade of MSS, Cr17Ni4 precipitation hardening stainless steel (17-4 PH stainless steel) possessed excellent mechanical properties and excellent corrosion resistance [4–7] induced by the precipitation of dispersed Cu-enriched particles in the martensite matrix. While, certain volume fraction of δ-ferrite had inevitably been introduced into the microstructure of the 17-4 PH stainless steel due to the chemical composition design of addition of Cr, which seriously deteriorated the thermo-plasticity of the alloy, and it was difficult to make the 17-4 PH stainless steel applicable to the large forging fields [8–10]. Toward to this limitation associated to the application of 17-4 PH stainless steel, a novel steel grade named Cr15Ni5 precipitation hardening stainless steel (15-5 PH stainless steel) was successfully developed on the basis of 17-4 PH stainless steel by increasing Ni content and reducing Cr content, and the δ-ferrite could be effectively reduced or eliminated in the final microstructure.

Domestic and foreign scholars had performed certain researches [11–13] concerning to MSS on the effect of aging process on the evolution of microstructure and mechanical properties. Wang et al. [11] investigated the effect of hardening behavior of 17-4 PH stainless steel aged at 350 °C for different time, and suggested the achieved microstructure was consisted of lath martensite and ε-Cu precipitates. The microstructure evolution of 17-4 PH stainless steel was reported by Murayama et al. [12], and it was proposed that Cu-enriched precipitates were formed on the martensite matrix after aging at 580 °C for 4 h. Sathyanath et al. [13] studied the microstructure evolution and strain hardening behavior of 17-4 PH stainless steel aged at 480 °C, 550 °C and 620 °C, respectively, and it was demonstrated that the strength of sample aged at 480 °C for 1 h was higher compared to others due to finer lath structure and higher density of dislocation. In summary, studies associated to the microstructure evolution discipline or aging process of 17-4 PH stainless steel have been paid a great

* e-mail: jhzhao2010@163.com

Table 1. Chemical composition of 15-5PH stainless steel (wt.%).

Element	C	Si	Mn	S	P	Cr	Ni	Mo+Nb	Cu	N	O	Fe
wt.%	0.04	≤1.00	≤1.00	≤0.01	≤0.03	14.2	3.5	0.5	2.50	≤0.01	≤0.01	Bal.

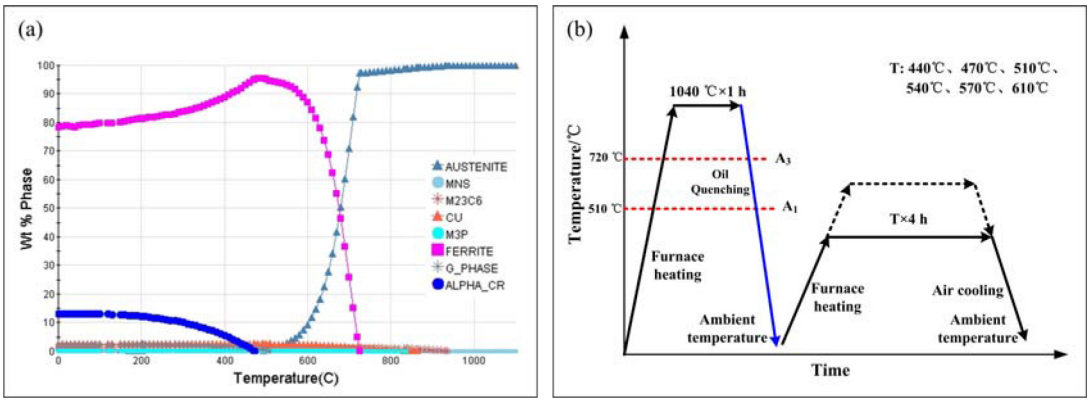

Fig. 1. (a) Equilibrium transition phase diagram of studied 15-5 PH stainless steel calculated by J-mat Pro, and (b) schematic diagram of heat treatment process.

attention from scholars, while corresponding investigations associated to 15-5 PH stainless steel was reported rarely. Zhou et al. [14] investigated the formation mechanism of Cu precipitation involved in the formation of reversed austenite by utilizing atom probe tomography, in situ synchrotron X-ray diffraction together with the thermodynamics and kinetics analysis, and the transformation pathway of reversed austenite and the precipitation generation mechanism were fundamentally revealed with respect to typical 15-5 PH stainless steel. Whereas, the other existing reports concerning to 15-5 PH stainless steel mainly focused on the investigation of fatigue and fracture properties [15–18]. It is necessary to clarify the basic influence of aging process on the evolution of microstructure and mechanical properties for further development of 15-5 PH stainless steel.

In present study, we focus on the effect of aging temperature on the evolution of microstructure and mechanical properties with regard to typical 15-5 PH stainless steel, and strengthening mechanisms involved in the specimens processed by different aging temperatures are further systematically explored, which are regarded as an experimental and theoretical foundation for the further industrial applications of 15-5 PH stainless steel.

2 Material and experimental procedure

2.1 Material and heat treatment

The material used in present study was 15-5 PH stainless steel, which was prepared in a 50 kg vacuum induction melting furnace. Ingot was forged into a slab with thickness of 100 mm utilizing press with 500 tons rated load after two rounds of upsetting and drawing process, and the initial forging temperature and final forging temperature were selected as 1160–1200 °C and 800–850 °C, respectively. The concrete chemical composition was shown in Table 1. To eliminate the inhomogeneity of microstructure and elements of the slab, homogenizing heat treatment was firstly performed at 950 °C for 5 h after the ingot was forged into slab. Then, the slabs were machined into specimens with dimension of 20 mm × 20 mm × 150 mm after homogenization, and solution and aging treatment process was adopted in present study. To guarantee the alloy elements could be soluted sufficiently, rational solution temperature and time were confirmed in accordance with reported studies [19], and the solution temperature and time were determined to be 1040 °C and 1 h, respectively. Similarly, it was reported that 4 h at least was needed for fast generation of Cu-enrichment precipitates in terms of the discipline of typical maraging stainless steel [19], and the aging time was confirmed to be 4 h in present study. To determine the critical transition temperature of the studied alloy, equilibrium transition phase diagram of the studied 15-5 PH was also calculated by utilizing thermodynamic software J-mat Pro, and the obtained phase diagram was depicted in Figure 1a. The aging temperature in present study was selected in the temperature range from 440 °C to 610 °C with interval of ~30 °C indicating aging was performed both in single α phase region or dual phase region including α and γ in terms of the calculated critical temperatures, and the schematic diagram of heat treatment and corresponding parameters were given in Figure 1b.

2.2 Mechanical property testing

Samples were processed into standard tensile samples after aging at different temperatures according to the specification GB/T228.1-2010 in China. The tensile tests were carried out at ambient temperature by utilizing an universal material tester (Model: Instron 5887) with tensile

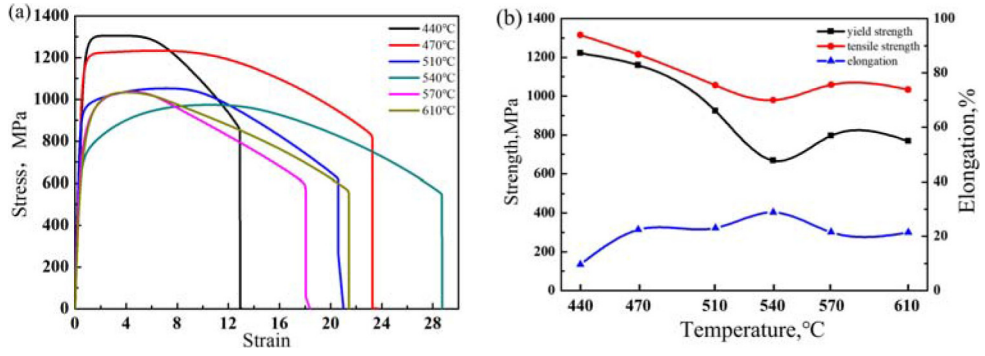

Fig. 2. (a) Tensile curves of studied 15-5 PH stainless steel processed by different aging temperatures, and (b) variation trend of mechanical properties as a function of aging temperature.

speed of 2 mm/min. 3 specimens were prepared and tested per aging process, and the mean value were determined to be the final mechanical properties.

2.3 Microstructural characterization

Specimens with size of 10 mm × 7 mm × 6 mm were cut from samples achieved by different aging processes. After mechanically grinding and polishing, the samples were corroded with ferric chloride solution (10 g $FeCl_3$ + 30 mL HCl + 40 mL H_2O) for 60 s, and then the metallographic structure was observed using an optical microscope (OM). The substructure of 15-5 PH stainless steel played an important role in determining the final mechanical property, and transmission electron microscope (TEM, model: JEM-2100) was applied to analyze the martensite substructure and precipitates. Specimens with thickness of 500 μm were mechanically polished to 40 μm, and punched into a disc with diameter of 3 mm. Samples then were thinned by using twin-jet polishing with solution consisted of 10% perchloric acid and 90% alcohol. Grain boundary with high-angle misorientation was generally used as an indicator of fine grain strengthening, and electron backscatter diffraction (EBSD) analysis was used to detect the distribution of various kinds of grain boundary. EBSD analysis was performed on a field emission scanning electron microscopy (model: Oxford) after electro-polished with 10% perchloric acid (polishing voltage: 30 V, polishing time: 30 s, step size: 0.2 μm). The experimental data was post-processed by HKL Channel 5 software to obtain crystallographic information such as the volume fraction of grain boundary, effective grain size as well as kernel average misorientation (KAM) information. To detect the volume fraction of retained austenite in the studied 15-5 PH stainless steel processed by different aging temperatures, X-ray diffraction (XRD) analysis was performed with step size of 0.04°. After mechanical polishing, electro-polished with 10% (volume fraction) perchloric acid alcohol electrolyte was used to remove the stress layer on the specimen surface induced by deformation. The XRD analysis was performed with Cu target on a X-ray diffractometer (model: Rigaku D/Max-2250VB/PC), and the scanning angle range was 40–120°.

3 Results and discussion

3.1 Mechanical properties

Typical tensile properties of 15-5 PH stainless steel aged at different temperatures were shown in Figure 2, and there were obvious differences between the samples processed by different aging processes. As can be seen from the stress-strain relation that the tensile curve of the 15-5 PH stainless steel was characterized by typical House-type curve, shown in Figure 2a, and there was no obvious yield platform. Hence, $R_{P0.2}$ was used as the yield strength value in present study. Figure 2b shows the variation of mechanical properties as a function of aging temperature with regard to the studied 15-5 PH stainless steel. It could be seen that the yield strength and tensile strength of the material were both decreased with the rise of aging temperature from 440 °C to 540 °C. The strength at 540 °C was lowest, at which the yield strength and tensile strength were determined to be 667 MPa and 979 MPa, respectively. When the temperature was further increased from 540 °C to the temperature 610 °C, the variation trend of the strength including yield strength and tensile strength nearly keep the wavy trend, and the strength were firstly increased followed by decreased slightly. Besides, it was noted that the variation trend of elongation was closely associated to the variation trend of strength, and the elongation and strength nearly kept ambivalent relations. The high strength generally corresponded to relative low ductility, and the low strength corresponded to relative high ductility. The maximum of elongation was determined to be 28.8% at aging temperature of 540 °C.

3.2 Effect of aging temperature on microstructural evolution

The optical micrographs of the studied 15-5 PH stainless steel aged at different temperatures were shown in Figure 3, and it could be seen that the microstructure of the 15-5 PH stainless steel was predominantly composed of martensite. While the morphology of the lath, precipitates and other microstructure information could not be characterized due to the small resolution of the optical microscope. In order to

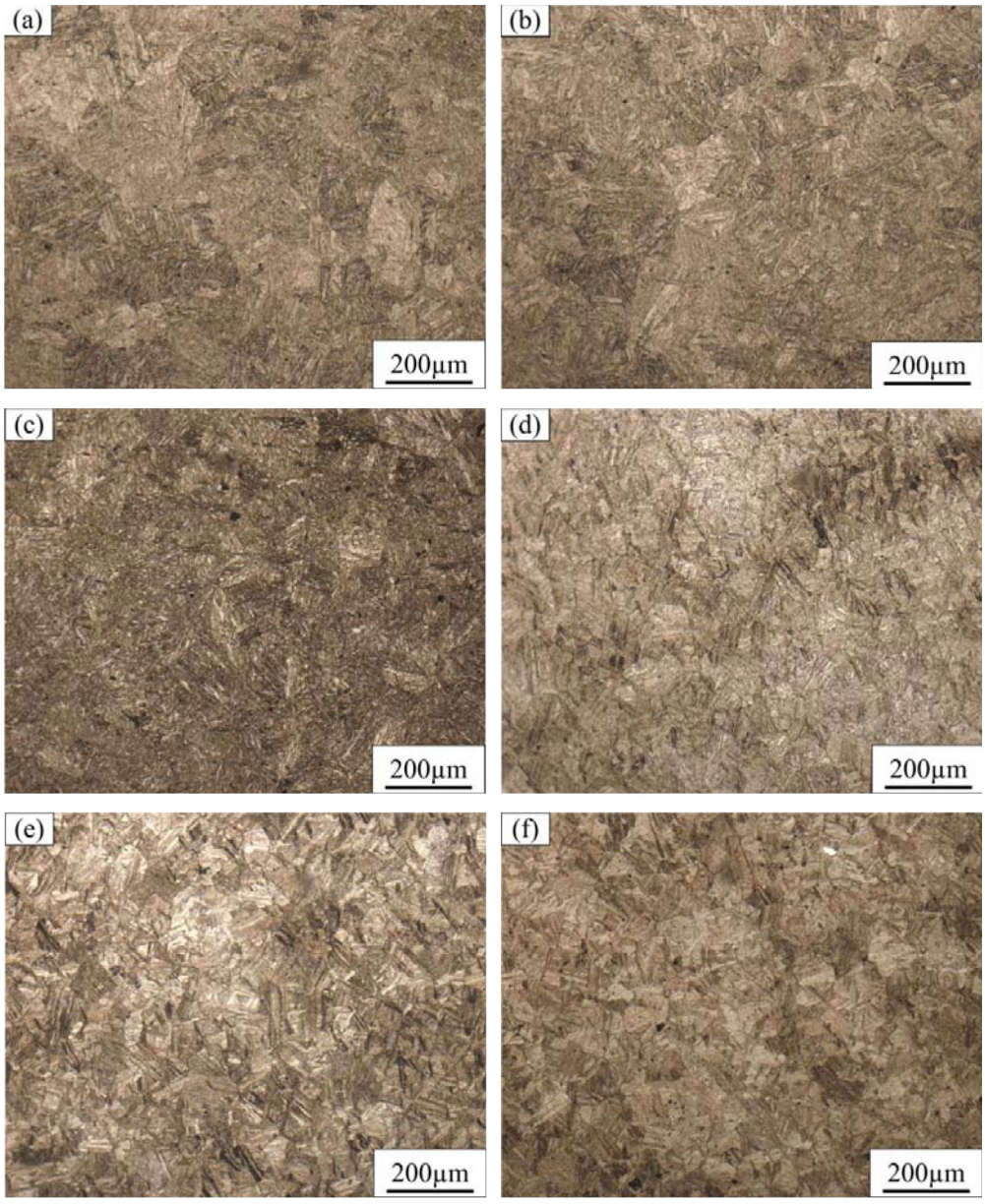

Fig. 3. OM micrographs aged at different temperatures. (a) 440 °C, (b) 470 °C, (c) 510 °C, (d) 540 °C, (e) 570 °C, and (f) 610 °C.

observe the substructure of the studied alloys processed by different aging temperatures, specimens were further analyzed by TEM, and the morphology of martensite lath of the studied alloys processed by different aging temperatures were depicted in Figure 4. Figure 4 shows that the substructure micrographs of the samples aged at 470 °C, 540 °C and 610 °C, respectively. It could be seen that the substructure of the studied 15-5 PH stainless steel processed by different aging temperatures was mainly composed of lath martensite, and dislocation cell with different morphologies could also be easily observed. The size of martensite lath distributed in the range from 106 nm to 289 nm at the aging temperature of 470 °C, and was increased to the range of 124–347 nm with aging temperature increased to 540 °C. When the aging temperature was further increased to 610 °C, the minimum of martensite lath was increased to 142 nm, and the largest width was increased to 416 nm. In accordance with the concrete heat-treatment process, it could be estimated that the size increment of martensite lath was attributed to the continuous migration of carbon atoms in martensite matrix to austenite with increasing aging temperature [20]. Besides, the morphology and number of dislocation cell were also locally decreased with the increase of aging temperature shown in Figure 4, which inevitably led to decrease of alloy strength [21].

Generally, Cu-enriched precipitates distributed on the ferrite matrix was the predominant cause contributing to high strength for typical strain hardening stainless steel [22,23]. In present study the features of the secondary phase

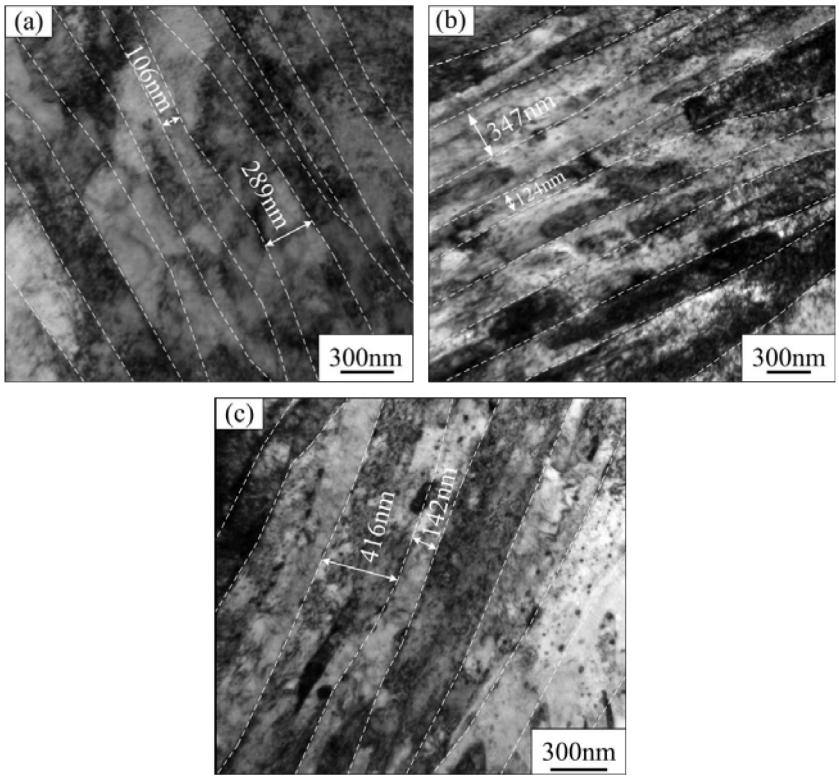

Fig. 4. TEM micrographs aged at different temperatures. (a) 470 °C, (b) 540 °C, and (c) 610 °C.

precipitates obtained by different aging processes were systematically characterized through TEM technique. Figure 5 further shows the precipitation morphology of alloys processed by different aging temperatures. As can be observed from Figure 5a, there was no precipitate in the matrix at the aging temperature of 470 °C. When the aging temperature was increased to 540 °C shown in Figure 5b, some Cu-enriched precipitates could be observed on the matrix in addition to certain dislocations cell, and the average size of the Cu-enriched precipitates was about 11.7 nm. In accordance with the reported studies [24,25], these Cu-enriched precipitates firstly formed a BCC structure, which kept coherent relation with matrix. Then the crystallographic structure of the precipitates was transformed into twin-9R structure from BCC, and finally transformed into FCC structure. When the aging temperature was further increased to 610 °C, it could be seen the volume fraction of dislocation cell was locally decreased, and the volume fraction of Cu-enriched precipitates with radius size below 25nm was larger compared to the sample aged at 540 °C, shown in Figure 5c. Eight TEM micrographs per aging process were counted to obtain the distribution information of precipitates, as shown in Figure 6, and the size of precipitates were mainly distributed in the range of 0–25 nm. It was accepted that the Cu-enriched precipitates keeping coherent relation with the martensite matrix was inclined to form a strain field [26], which can effectively pin the movement of dislocations during deformation and increase the strength of the alloy. Hence, it can be indicated that Cu-enriched precipitates appearing in present alloy aged at temperatures of 540 °C and 610 °C can act as the potential role for strength improvement.

3.3 Strengthening mechanism at different aging temperatures

As can be seen from the mechanical property variation discipline shown in Figure 2, the strength of the studied 15-5 PH stainless steel decreased firstly and then increased with increasing aging temperature, and the elongation nearly kept contradictory relation with the strength. The variations of mechanical properties including the strength and elongation under different aging processes were closely associated to the microstructure, and were further attributed to the contribution induced by different strengthening mechanisms. Generally, the classical strengthening mechanisms including solid solution strengthening, fine grain size strengthening, dislocation strengthening as well as precipitation strengthening were potential for the studied 15-5 PH stainless steel, and the role of different strengthening mechanisms contributing to strength increment were predominantly attributed to the different aging processes. For solid solution strengthening, the interstitial solid solution elements such as C and N were responsible for the strength increment. Considering the relative low-carbon chemical composition design for the studied 15-5 PH stainless steel, influence of interstitial elements on the strength increment under aging temperature range

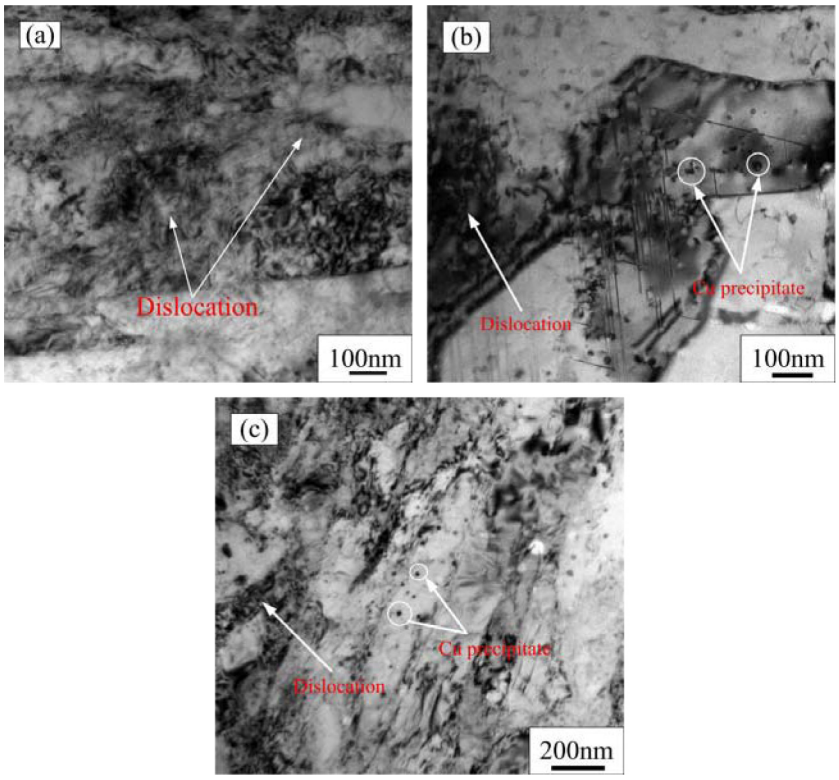

Fig. 5. TEM micrographs aged at different temperatures. (a) 470 °C, (b) 540 °C, and (c) 610 °C.

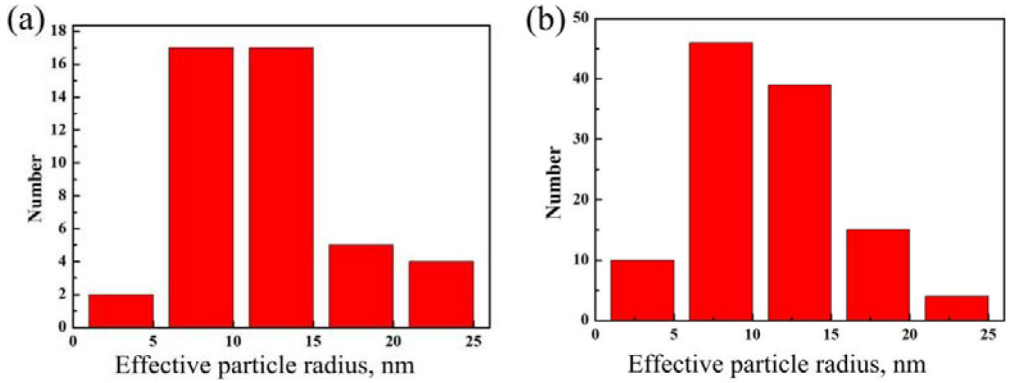

Fig. 6. Distribution of effective particle size with respect to studied 15-5 PH stainless steel processed at aging temperature of (a) 540 °C, and (b) 610 °C.

of 440–610 °C could be ignored. In order to clarify the strength contribution induced by fine grain size strengthening at different aging temperatures, the crystallographic orientation information was achieved through EBSD, and the inverse pole figure (IPF) mapped figures of the studied alloys processed by different aging temperatures were depicted in Figure 7. The volume fractions of low-angle grain boundary (LAGB) and high-angle grain boundary (HAGB) were generally used as an indicator reflecting the hidden effects to dislocation slip during deformation, which could be further regarded as fine grain size strengthening. For the studied 15-5 PH stainless steel, the volume fractions of LAGB and HAGB were statistics as shown in Figure 7g, and the volume fractions of LAGB and HAGB varied slightly with the increase of aging temperature from 440 °C to 610 °C, indicating fine grain size strengthening was not responsible for the variation discipline of mechanical properties under different aging temperatures with respect to the studied 15-5 PH stainless steel.

As depicted in Section 3.2, the martensite lath with certain dislocation cell and Cu-enriched precipitation could be observed on the substructure of the studied 15-5 PH stainless steel processed by different aging temperatures.

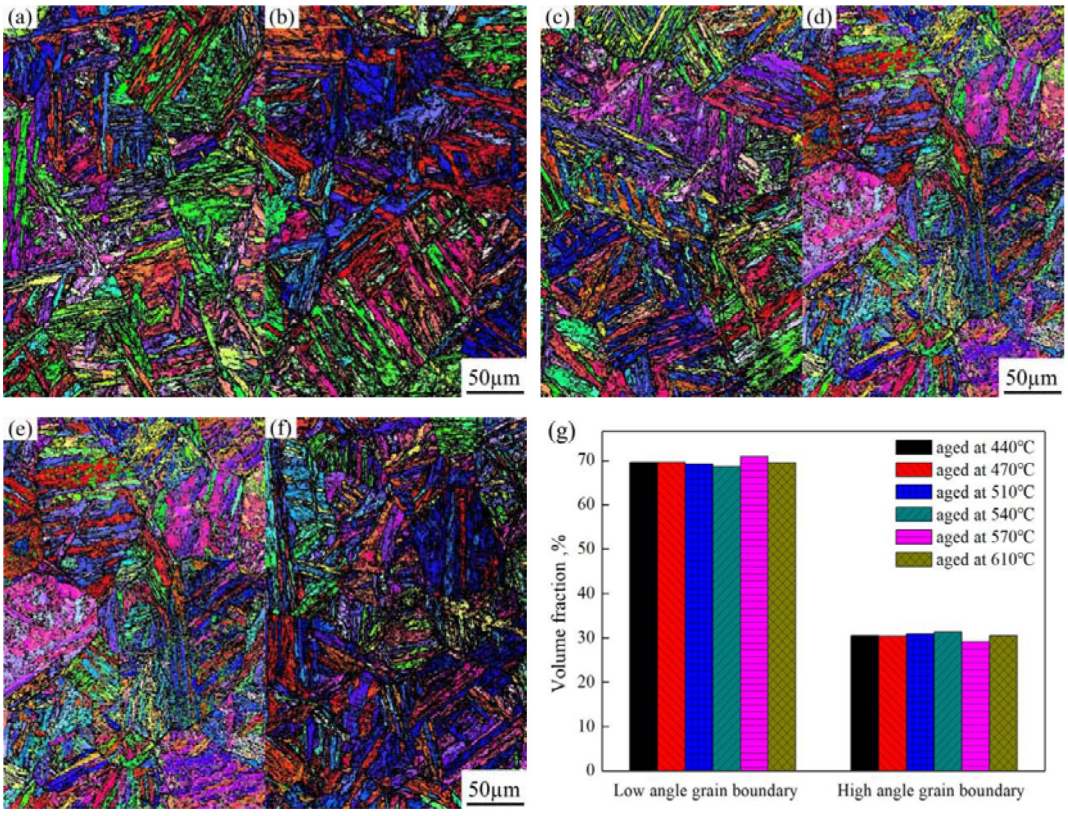

Fig. 7. IPF mapped figure of studied 15-5 PH stainless steel aged at temperature of (a) 440 °C, (b) 470 °C, (c) 510 °C, (d) 540 °C, (e) 570 °C, and (f) 610 °C; (g) distribution statistic of HAGB and LAGB.

Therefore, it could be concluded the strengthening mechanisms determining the variation discipline of mechanical properties with regard to the studied 15-5 PH stainless steel predominantly included precipitation strengthening and dislocation strengthening. These two strengthening mechanisms were mainly related to the size and volume fraction of precipitated particles and the number of dislocation cell. For precipitation strengthening, it was clearly to understand the relations between strengthening mechanism and the aging process. With the increase of aging temperature, the Cu-enriched precipitates appeared and became coarsen gradually. When the aging temperature was 470 °C, Cu-enriched precipitates did not appear and had no strengthening on the material matrix, and dislocation strengthening was dominant at this circumstance. When the aging temperature was increased to 540 °C, certain volume fraction of Cu-enriched precipitation was generated and distributed on the martensite matrix, which strengthen the alloy through Orowan strengthening mechanism. It was reported the crystal lattice of Cu-enriched precipitation was different from the martensite matrix [24]. When the dislocation cut through the particles, extra energy was needed to overcome the energy of atomic disarrangement on the slip plane, which contributed to increment of strength. The stress field induced by precipitates would impede the movement of the dislocation, and the activation energy for the movement of dislocation would be increased to achieve the strengthening effect. When the aging temperature was further increased to 610 °C, the volume fraction of Cu-enriched precipitates at aging temperature 610 °C was further increased greatly compared to 540 °C, shown in Figure 6, indicating the strengthening effect induced by precipitation was further improved. Hence, it can be concluded the strengthening contribution induced by Cu-enriched precipitation was gradually increased with aging temperature increasing from 540 °C to 610 °C with respect to studied 15-5 PH stainless steel. When taking the dislocation strengthening into account, it was more complex to understand the relations between dislocation strengthening mechanism and the aging process due to the formation of reverted austenite during aging process. Generally, it was commonly believed that the width of martensite lath became wider and the density of dislocation was decreased due to the recovery mechanism with increasing aging temperature. Whereas, there was a reverse phase transition from martensite to the γ phase at certain aging temperature with respect to the studied 15-5 PH stainless steel in accordance with the equilibrium transition phase diagram shown in Figure 1, and the effects induced by reverted austenite on the mechanical properties with regard to studied 15-5 PH stainless steel could not be neglected. Once reverted austenite could be kept stably in ambient temperature, the strength of the studied 15-5 PH stainless steel could be decreased seriously. It had also been verified in literature [27] that formation of reverted

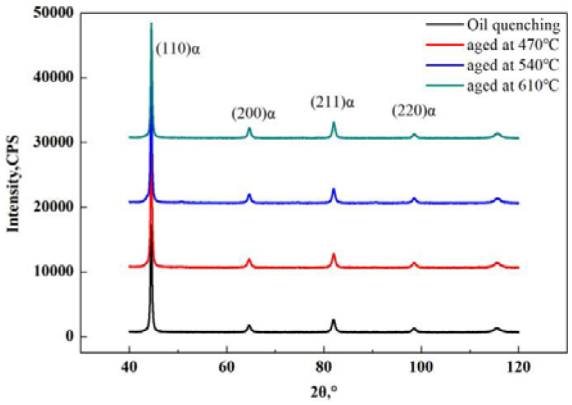

Fig. 8. XRD spectrum of studied 15-5 PH stainless steel aged at different temperatures.

austenite during aging process sometime would lead to the decrease of strength with regard to some precipitation hardening stainless steel. On the contrary, the unstable reverted austenite initiated in the high temperature dual-phase region then transformed into fresh martensite upon cooling when the final temperature was below Ms. Then the high density of dislocation induced by fresh martensite could contribute to the increment of strength, indicating dislocation strengthening mechanism is responsible for the strength increment at this condition.

In this study, to detect the volume fraction of retained austenite in the studied 15-5 PH stainless steel processed by different aging temperatures ranging from 470 °C to 610 °C, the X-ray diffraction spectrum and calibration of the 15-5 PH stainless steel aged at different temperatures were shown in Figure 8. When the 2θ varied in the range of 40–120°, diffraction peaks induced by $(110)_\alpha$, $(200)_\alpha$, $(211)_\alpha$, $(220)_\alpha$ crystallographic planes could be obviously observed. While, any diffraction peak induced by typical crystallographic plane of FCC structure could not be found, indicating there was no stable retained austenite residual in the microstructure processed by different aging temperatures, and the variation discipline in strength induced by reverted austenite could be neglected. Furthermore, the KAM method was utilized to analyze the dislocation distribution of the studied 15-5 PH stainless steel processed by typical aging temperatures. The KAM was a measure of local grain misorientation that was usually derived from EBSD data, and it had been accepted the KAM results could reflect the distribution of dislocation density associated to local region. On the basis of the dual-phase region determined by the equilibrium transition phase diagram as shown in Figure 1, the aging temperature ranging from 540 °C to 610 °C was located in the dual-phase region, and the KAM information of the studied 15-5 PH stainless steel processed at aging temperature ranging from 540 °C to 610 °C was depicted in Figure 9, where the white represents the unrecognized region, the blue represents the local region with low dislocation density, and the green represents the region with high dislocation density. It could be achieved that the dislocation distribution represented by green area was uneven, and certain volume fraction of dislocations was distributed on the local matrix. Based on the dislocation initiation mechanism from fresh martensite, this kind of unevenly distributed dislocation was transformed from the unstable reverted austenite initiated in the dual-phase region during aging process, which further played significant role in improving strength of the 15-5 PH stainless steel.

In summary, the corresponding relations between the variation discipline of strength and the various strengthening mechanisms as a function of aging temperature for the studied 15-5 PH stainless steel were schematically depicted in Figure 10. As can be observed from Figure 10, solid solution strengthening and fine grain size strengthening were not the predominant strengthening mechanisms contributing to variation discipline of mechanical properties with regard to the studied 15-5 PH stainless steel, and the variations of properties were mainly attributed to the dislocation strengthening and precipitation strengthening. For the studied 15-5 PH stainless steel processed at the aging temperature range of 440–540 °C, the dislocation strengthening was dominated in addition to solid solution and fine grain size strengthening, and the precipitation strengthening could be ignored. While, the coupling effect of precipitation strengthening and dislocation strengthening was acted in addition to constant solid solution and fine grain size strengthening, and the precipitation strengthening and dislocation strengthening were dominated for the studied 15-5 PH stainless steel processed at the aging temperature ranging from 540 °C to 610 °C.

4 Conclusion

- The tensile strength of the studied 15-5PH stainless steel was decreased with the rise of aging temperature from 440 °C to 540 °C. When the temperature was further increased from 540 °C to the temperature 610 °C, the variation trend of the strength including yield strength and tensile strength nearly kept the wavy trend, and the strength were firstly increased followed by decreased slightly. Besides, the elongation and strength nearly kept ambivalent relations in the whole aging temperature range of 440 °C to 610 °C.
- The microstructure of the studied 15-5 PH stainless steel was predominantly composed of lath martensite with certain volume fraction of dislocation in the aging temperature range of 440 °C to 610 °C, and the width of martensite lath was increased with the rise of aging temperature. Besides, some Cu-enriched precipitates appeared in the material when the aging temperature was above 540 °C, and the volume fraction of Cu-enriched precipitates was also increased with the increasing aging temperature.
- There was almost no austenite residual with regard to the studied 15-5 PH stainless steel processed by different aging temperatures, and the dislocation strengthening was dominated in addition to solid solution and fine grain size strengthening at the aging temperature range of 440 °C to 540 °C. While, the precipitation strengthening was dominated for the studied 15-5 PH stainless steel processed at the aging temperature range of 540–610 °C.

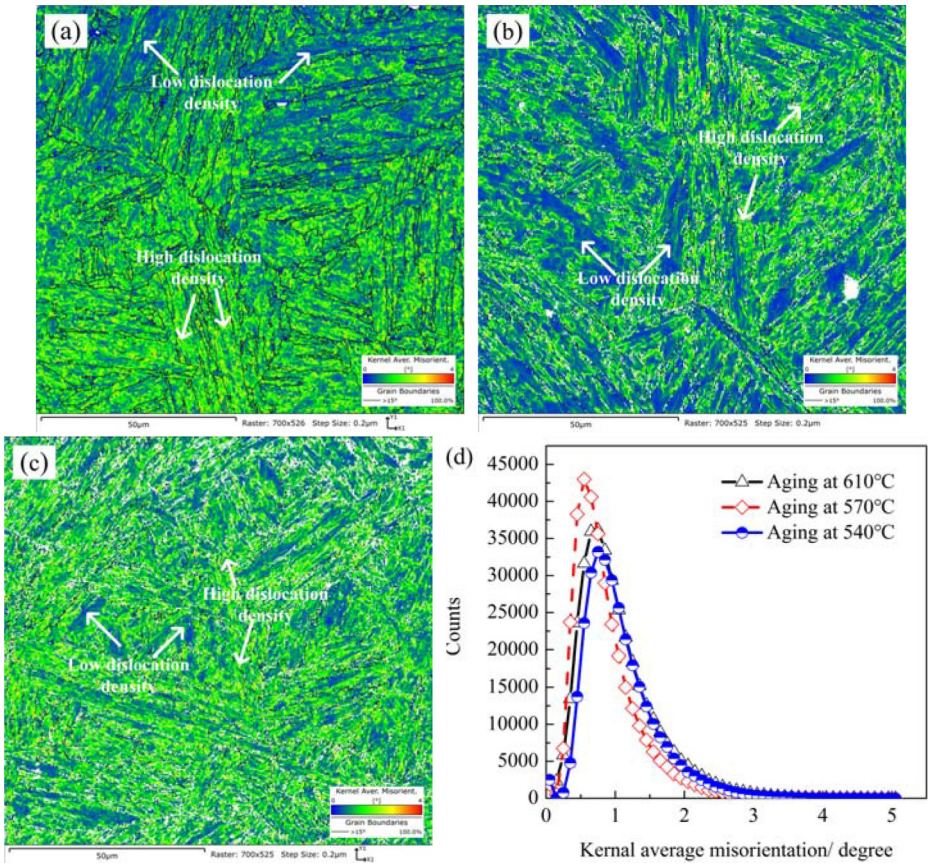

Fig. 9. KAM information of studied 15-5 PH stainless steel processed at aging temperature of (a) 610 °C, (b) 570 °C, (c) 540 °C, and (d) distribution of misorientation.

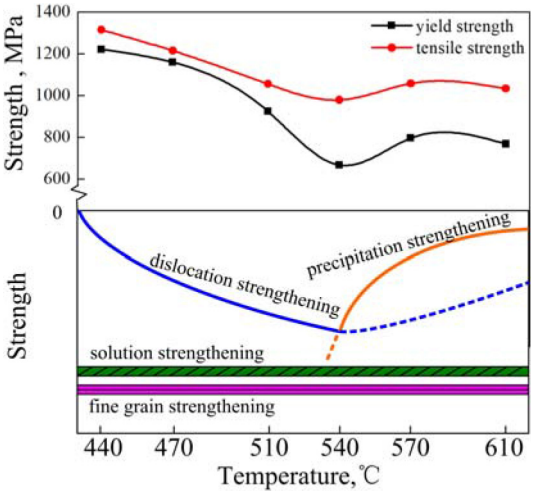

Fig. 10. Schematic diagram of correlations between mechanical property variation discipline and strengthening mechanisms.

Acknowledgements. The authors acknowledge the financial supports from "Taiyuan University of Science and Technology Scientific Research Initial Funding (No. 20182007)", and "Applied Basic Research Program in Shanxi, China (No. 201901D211309)". J.H Zhao also appreciates the beneficial discussion with doctor candidate Mr. D Liu in State Key Laboratory of Rolling and Automation (RAL), China, about KAM theory.

References

1. J. Wang, H. Zou, L. Cong, Int. J. Min, Met Mater. **13**, 235–239 (2006)
2. L.E. Murr, E. Martinez, J. Hernandez et al., J. Mater. Res. Technol. **1**, 167–177 (2012)
3. D. Guo, T.K. Chi, L.M. Tam et al., Surf. Coat. Technol. **402**, 126302 (2020)
4. U.K. Viswanathan, S. Banerjee, R. Krishnan, Mater. Sci. Een. A **104**, 181–189 (1988)
5. J. Tian, W. Wang, W. Yan et al., Eng. Fail. Anal. **65**, 57–64 (2016)
6. L. Xin, Y. Cao, X. Wu et al., Mater. Sci. Eng. A **553**, 80–88 (2012)
7. A.R. Etemadi, P. Behjati, A. Emami, Eng. Fail. Anal. **18**, 1242–1246 (2011)
8. J. Srinath, S.K. Manwatkar, S. Murty, J. Mater. Eng. Perform. **4**, 29–44 (2015)
9. H.J. Rack, D. Kalish, Metall. Mater. Trans. B **5**, 1595–1605 (1974)
10. R. Hamlin, J. Dupont, Metall. Mater. Trans. A **48**, 1–19 (2016)

11. J. Wang, H. Zou, L. Cong, Mater. Charact. **57**, 274–280 (2006)
12. M. Murayama, K. Hono, Y. Katayama, Metall. Mater. Trans. A **30**, 345–353 (1999)
13. A. Sathyanath, A. Meena, Mater. Today. Commun. **25**, 101416 (2020)
14. T. Zhou, B. Neding, S. Lin et al., Scr. Mater. **202**, 114007 (2021)
15. Z. Sun, C. Moriconi, G. Benoit, Metall. Mater. Trans. A **44**, 1320–1330 (2013)
16. A. Spierings, T. Starr, K. Wegener, Rapid. Prototyping. J. **19**, 88–94 (2013)
17. L. Jikai, M. Coret, A. Combescure et al., Combescure, Eng. Fract. Mech. **96**, 328–339 (2012)
18. K. Abhay, K. Sreekumar, P.P. Sinha, Eng. Fail. Anal. **17**, 1195–1204 (2010)
19. X.Y. Peng, X.L. Zhou, X.Z. Hua et al., J. Iron. Steel. Res. Int. **22**, 607–614 (2015)
20. P. Du, P. Chen, D.K. Misra, Metals-Basel. **10**, 1343 (2020)
21. A. Ning, S. Yue, R. Gao et al., Metals-Basel **9**, 1283 (2019)
22. J. Wang, H. Zou, C. Li, Mater. Charact. **59**, 587–59 (2008)
23. R. Bhambroo, S. Roychowdhury, V. Kain, Mat. Sci. Eng. A-Struct. **568**, 127–133 (2013)
24. R. Monzen, M. Jenkins, A. Sutton, Philos. Mag. **80**, 711–723 (2000)
25. B.L. Tiemens, A.K. Sachdev, Metall. Mater. Trans. A **43**, 3615–3625 (2012)
26. A. Kumar, Y. Balaji, N.E. Prasad et al., Sadhana-Acad. P. Eng. S. **38**, 3–23 (2013)
27. C.N. Hsiao, C.S. Chiou, J.R. Yang, Mater. Chem. Phys. **74**, 134–142 (2002)

Cite this article as: Chunhui Jin, Honglin Zhou, Yuan Lai, Bei Li, Kewei Zhang, Huiqin Chen, Jinhua Zhao, Microstructure and mechanical properties of 15-5 PH stainless steel under different aging temperature, Metall. Res. Technol. **118**, 601 (2021)